



# Analysis of Surfaces Characteristics Stability in Grinding Process

Naoufel Ben Moussa<sup>(✉)</sup>, Nasreddine Touati, and Nabil Ben Fredj

Laboratoire de Mécanique, Matériaux et Procédés LR99ES05,  
Ecole Nationale Supérieure d'Ingénieurs de Tunis, Université de Tunis,  
5 Avenue Taha Hussein, Montfleury, 1008 Tunis, Tunisia  
emailnaoufel@gmail.com, benfredjnabil@gmail.com,  
touatinasr@yahoo.com

**Abstract.** In this work, we investigate the effect of the grinding wheel morphology at grain scale on the stochastic aspects of the process. This morphology was controlled through dressing conditions in order to optimize the ground surface characteristics while minimizing their variance. It has been found that under the same grinding conditions, the surface characteristics and their dispersion vary significantly according to the dressing parameters. For the case of the grinding wheel (95A46M6V) dressed by a single-point diamond, a good choice of dressing conditions allows to reduce the roughness from 2 to 0.76  $\mu\text{m}$  with a scatter less than 10% and to increase the hardening from 220Hv with a scattering of 40% to 382Hv with a dispersion of 23%.

**Keywords:** Grinding · Stainless steel · Surface properties · Wheel topography · Scatter

## 1 Introduction

The grinding process, and despite its efficiency in terms of dimensional and geometric accuracy of finished parts, is not sufficiently controlled owing to the large number of dispersion sources resulting mainly from the stochastic nature of the grinding wheel morphology. The removal of material is performed by a multitude of cutting edges with random sizes, shapes, orientations and spatial distribution leading to different material removal mechanisms, which consequently affects dispersions on mechanical surface characteristics of ground parts (Liu and Yang 2001). The accurate identification of ground surface characteristics is required to enhance the aptitude of component life predictive models (Ben Moussa et al. 2014a, b; Sidhom et al. 2014a, b; Yahyaoui et al. 2015; Zouhayar et al. 2013). In most research work, the effects of dressing conditions have been quantitatively evaluated through the finished surface characteristics and cutting forces without investigation of the real grinding wheel topography after dressing (Hadad and Sharbati 2016; Inasaki and Okamura 1985; Puerto et al. 2013). Last years, the technical evolution of measurement and visualization equipment has made it possible to evaluate the topography of the wheel (Badger and Torrance 2000; Woodin 2014; Coelho et al. 2001; Darafon 2013; Hadad and Sharbati 2016; Xie et al. 2008; Kapłonek and Nadolny 2013). In literature reviews, several indicators have been

used to assess the grinding wheel topography at the microscopic scale. These indicators are commonly calculated from measurements made by contact and non-contact devices. The main obstacle often encountered in the investigation of the grinding wheel topography using the most of these devices is the requirement of the destruction of the wheel or its removal from the machine. In addition, in most research, the effects of grinding conditions on surface integrity have been established without studying the effects of dressing conditions on the stability of the ground surfaces characteristics. In this study, we propose an experimental methodology for investigating, on site, the effect of dressing conditions on the microscopic grinding wheel topography characteristics. This methodology is used to determine quantitative indicators of dispersions characterizing the grinding process. The analysis of ground surface characteristics for different dressing conditions allows improving the aptitude of the grinding process to remove material while reducing the scatter of ground surfaces characteristics by controlling the dressing parameters.

## 2 Experiments

### 2.1 Material

Grinding operations were carried out on samples of austenitic stainless steel AISI304 with dimensions  $15 \times 35 \times 8$  mm. The chemical composition and physical properties are given in Table 1. A stress-relief annealing treatment was applied to all samples to remove the anterior residual stresses (Fredj et al. 2006).

**Table 1.** Chemical composition and mechanical properties of the AISI 304 stainless steel.

C	Si	Mn	Cr	Ni	Mo	Cu	N	Fe
0.05	0.41	1.14	18.04	9	0.193	0.348	0.004	Bal- ance
E (GPa)		Rm (MPa)		Rp0.2 (MPa)		A (%)		Hardness Hv0.1
193		670		315		53		270

### 2.2 Experimental Setup

The dressing and grinding operations are carried out in this work on a Teknoscuola RT600 grinding machine having two automated axes in vertical and longitudinal directions. Experiments were conducted using a Norton 95A46M6V vitrified aluminum oxide grinding wheel. A motorized device was designed and mounted on the grinding machine for controlling the dressing speed in the transverse direction  $V_d$  (Fig. 1). An electronic dimmer (Altivar11) is used to vary the dressing speed between 0.5 mm/s and 10 mm/s. In this work, a single-point diamond dresser was used for truing the wheel and generating fresh cutting edges (Fig. 1).

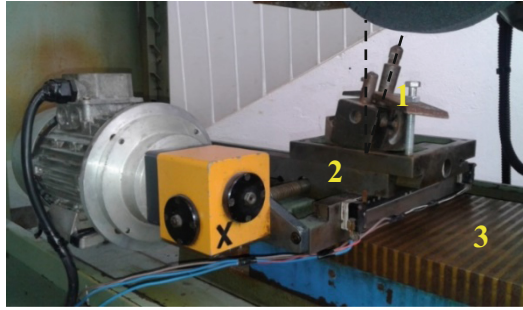


**Fig. 1.** Dressing feed variation device: dresser (1), trainer table (2), grinder magnet table (3)

The dressing conditions, summarized in Table 2, were chosen according to the specifications recommended by the wheel manufacturer (Norton). The speed of the spindle is kept constant during the dressing operations at a value of 2700 rpm. After each dressing condition three grinding passes ( $V_w = 5.7$  m/min,  $a_e = 30$   $\mu\text{m}$ ) are performed on the prismatic pieces of austenitic stainless steel AISI 304.

**Table 2.** Dressing conditions.

N°	1	2	3	4	5	6	7	8	9
Vd (mm/s)	1	1	1	5	5	5	10	10	10
ad ( $\mu\text{m}$ )	5	15	30	5	15	30	5	15	30

### 2.3 Examination of Grinding Wheel Surface

In this work, the characterization of the grinding wheel surface morphology is performed using a Carson MM-840 digital microscope type. For a magnification of 75x, ten zones of the grinding wheel with dimensions of  $5.71 \times 4.28$  mm were observed after each dressing condition. In this study, the cutting-edges density  $A$  (%) and the spatial distribution of cutting edges  $R$  are chosen as evaluation indicators of the grinding wheel topography. The differentiation of peaks and hollows in acquired micrographs requires a good positioning of the light source (Fig. 2a).

For the observed zone, about 100 high quality micrographs with a resolution of  $3200 \times 2400$  pixels were performed varying the angle of capture. These micrographs were processed using a freeware SFM (structure from motion) photogrammetry program (Wu 2013) to create a three-dimensional model of the observed zone. The intersection between the 3D model and a virtual plane distant from the highest point by the depth of pass  $a_e$  allows determining the active edges surface area (Fig. 2b). Thereafter, the image processing program ImageJ (Schneider et al. 2012) is used to determine the cutting-edge density by analyzing micrographs of 10 spaced zones of grinding wheel after each dressing or grinding operations. For this purpose, all colored micrographs are converted to gray scale picture where for each pixel a gray level between 0 and 255 is assigned. Thereafter, a binary segmentation process was applied

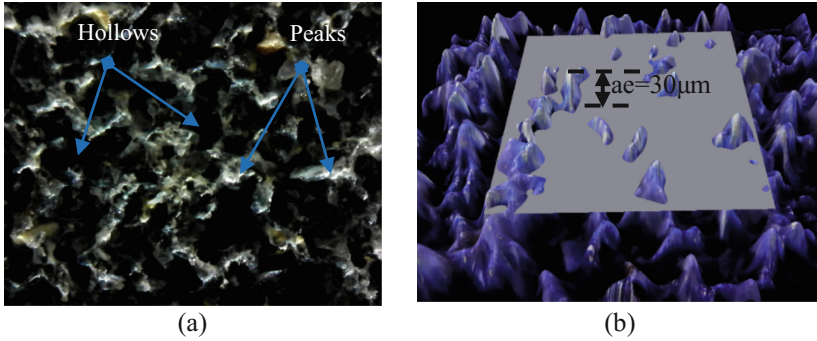


**Fig. 2.** Micro topography of grinding wheel

to all pixels to convert those with a gray level below a threshold to black and the others representing the distribution of the active edge to white. The threshold is determined after testing several thresholds and a value of 200 was chosen since it gives a value of active surface equal to that obtained from three-dimensional model.

### 2.3.1 Evaluation of Cutting-Edge Density and Spatial Distribution

Figure 4 shows the effect of dressing velocity  $V_d$  and dressing depth of pass  $a_d$  on cutting edge density. Coarse dressing (high  $a_d$  and  $V_d$  values) results in macrofractures of the grit and complete dislocations of grain blocks and coolant, which explains the decrease in the density of the cutting edges. On the other hand, the fine dressing (low  $a_d$  and  $V_d$  values) makes the surface of the grinding wheel more closed, which results in the appearance of a higher number of light areas in the micrographs, therefore an increase in the density of the active surfaces is obtained.

The spatial arrangement of active cutting edges is determined from their center coordinates using a code developed in this work and based on the nearest neighbor search method (Taylor 1977). Figure 3 shows a decrease of the spatial dispersion of the active edges  $R$  when dressing is carried out under coarse conditions. It is noted that the decrease of the dispersion index  $R$  depicts an accumulation of active surfaces due to grits fracture and stripping under high dressing velocity and depth of pass.

## 2.4 Evaluation of Workpiece Characteristics

### 2.4.1 Effect on the Stability of the Roughness Indicators

Figure 4 shows an increase of roughness ( $R_a = 2 \mu\text{m}$ ) when grinding wheel dressing is performed under coarse conditions. This effect is in agreement with the results found by (Hadad and Sharbati 2016) and (Puerto et al. 2013) when grinding a St37 mild steel and F-5229 steel, respectively with conventional alumina-grinding wheels dressed using a single tip dresser. In addition, roughness covariance is the highest (about 30%) for coarse dressing condition. This result can be explained by the increase in the heterogeneity of the grinding wheel morphology resulting from coarse dressing. For fine

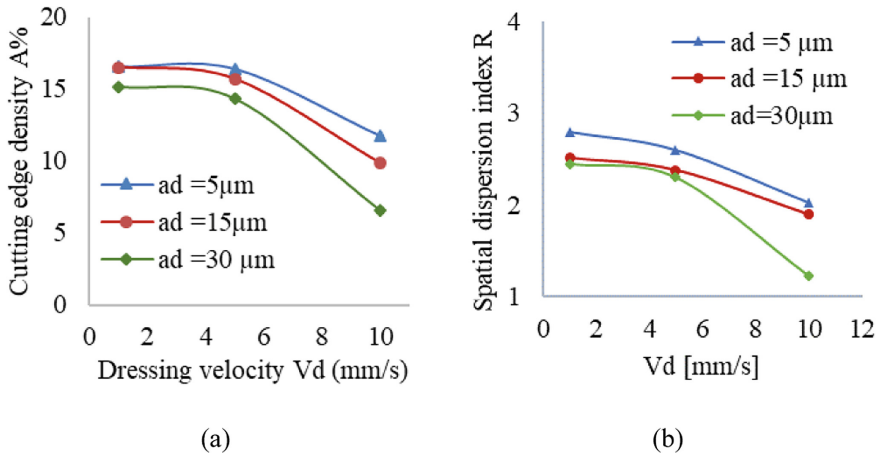


**Fig. 3.** Effects of dressing conditions on cutting edges: (a) density, (b) spatial dispersion

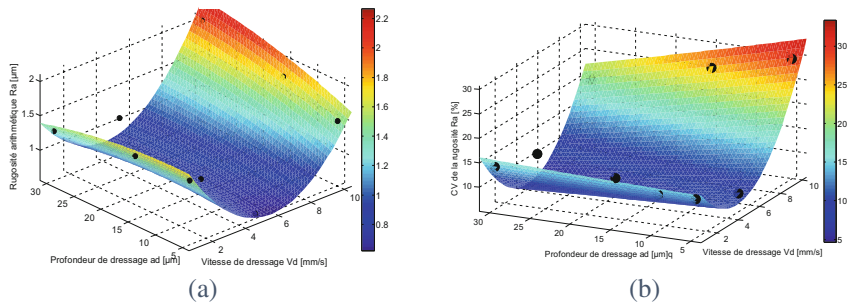


**Fig. 4.** Effect of dressing conditions on ground surface roughness values and dispersions

dressing condition, roughness value is decreased to  $0.76\ \mu\text{m}$  with a dispersion less than 15% due to the increase of the active edge density and the regularity of their spatial distribution on the grinding wheel surface.

#### 2.4.2 Effect on the Stability of the Microhardness Distribution

The analysis of spatial distributions of microhardness on the ground surfaces is carried out by performing grids of 100 indentations spaced by  $50\ \mu\text{m}$  for all dressing conditions. The fine dressing conditions result in a smooth grinding wheel with dense active surfaces, which results in an increase of area interacting with the workpiece material. Figure 5 shows that fine dressing leads to an increase of averaged microhardness while minimizing its covariance. On the other hand, the coarse dressing condition leads to low microhardness average along with highest covariance.

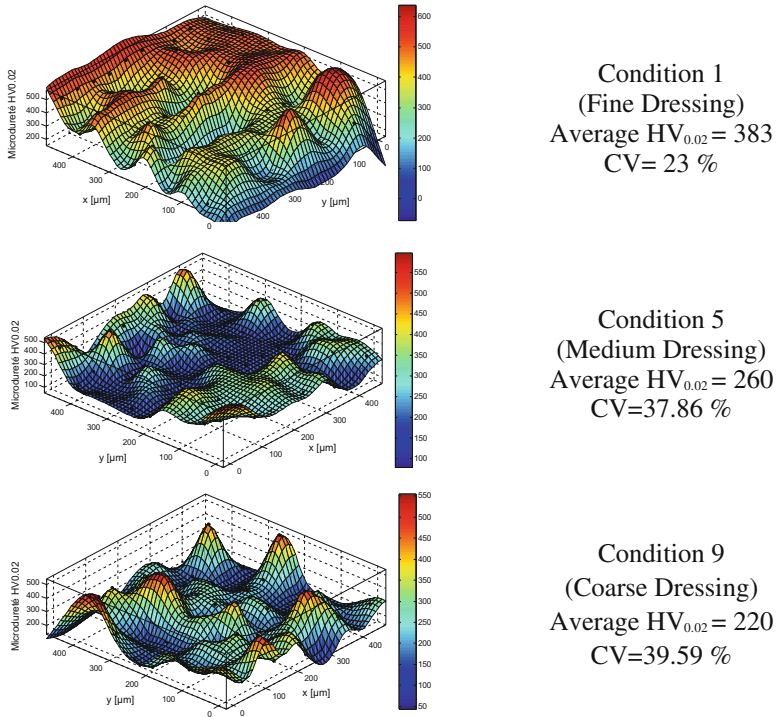


Fig. 5. Effect of dressing conditions on ground surface microhardness

### 3 Conclusion

The main objective of this study is to analyse the effect of the random aspect of the grinding process on ground surface characteristics and their stability.

A new method for characterization of the grinding wheel morphology and its ability to remove material has been proposed. This method is based on the acquisition and analysis of micrographs in real-time in different areas of the wheel that allowed determining the density of active surfaces and their spatial dispersion.

The grinding wheel morphology is successfully controlled by mean of dressing conditions allowing a significant enhancement of the distribution of surface roughness and hardness.

### References

- Badger, J., Torrance, A.: A comparison of two models to predict grinding forces from wheel surface topography. *Int. J. Mach. Tools Manuf.* **40**(8), 1099–1120 (2000)
- Ben Moussa, N., Al-Adel, Z., Sidhom, H., Braham, C.: Numerical assessment of residual stress induced by machining of aluminum alloy. *Adv. Mater. Res.* **996**, 628–633 (2014a). <http://doi.org/10.4028/www.scientific.net/AMR.996.628>

- Ben Moussa, N., Sidhom, N., Sidhom, H., Braham, C.: Prediction of cyclic residual stress relaxation by modeling approach. *Adv. Mater. Res.* **996**, 743–748 (2014b). <http://doi.org/10.4028/www.scientific.net/AMR.996.743>
- Coelho, R.T., De Oliveira, J.F.G., Marinelli Filho, N.: *The Application of Acoustic Emission (AE) Techniques on the Dressing Operation Using Synthetic Diamonds and Sintered Tools* (2001)
- Darafon, A.: *Measuring and Modelling of Grinding Wheel Topography*. Dalhousie University, Halifax (2013)
- Fredj, N.B., Djemaiel, A., Rhouma, A.B., Sidhom, H., Braham, C.: Effects of the cryogenic wire brushing on the surface integrity and the fatigue life improvements of the AISI 304 stainless steel ground components. In: Youtsos, A.G. (ed.) *Residual Stress and its Effects on Fatigue and Fracture*, Dordrecht, 2006, pp. 77–86. Springer, Netherlands (2006)
- Hadad, M., Sharbati, A.: Analysis of the effects of dressing and wheel topography on grinding process under different coolant-lubricant conditions. *Int. J. Adv. Manuf. Technol.* **90**, 1–12 (2016)
- Inasaki, I., Okamura, K.: Monitoring of dressing and grinding processes with acoustic emission signals. *CIRP Ann. Manuf. Technol.* **34**(1), 277–280 (1985)
- Kapłonek, W., Nadolny, K.: Assessment of the grinding wheel active surface condition using SEM and image analysis techniques. *J. Braz. Soc. Mech. Sci. Eng.* **35**(3), 207–215 (2013)
- Liu, C.R., Yang, X.: The scatter of surface residual stresses produced by face-turning and grinding. *Mach. Sci. Technol.* **5**(1), 1–21 (2001)
- Taylor, P.J.: *Quantitative Methods in Geography*, pp. 133–172. Waveland Press Inc., Prospect Heights (1977)
- Puerto, P., Fernández, R., Madariaga, J., Arana, J., Gallego, I.: Evolution of surface roughness in grinding and its relationship with the dressing parameters and the radial wear. *Procedia Eng.* **63**, 174–182 (2013)
- Schneider, C.A., Rasband, W.S., Eliceiri, K.W.: NIH image to ImageJ: 25 years of image analysis. *Nat. Methods* **9**, 671 (2012). <https://doi.org/10.1038/nmeth.2089>
- Sidhom, H., Ben Moussa, N., Ben Fathallah, B., Sidhom, N., Braham, C.: Effect of surface properties on the fatigue life of manufactured parts: experimental analysis and multi-axial criteria. *Adv. Mater. Res.* **996**, 715–721 (2014a). <http://doi.org/10.4028/www.scientific.net/AMR.996.715>
- Sidhom, N., Moussa, N.B., Janeb, S., Braham, C., Sidhom, H.: Potential fatigue strength improvement of AA 5083-H111 notched parts by wire brush hammering: Experimental analysis and numerical simulation. *Mater. Des.* **64**, 503–519 (2014b). <https://doi.org/10.1016/j.matdes.2014.08.002>
- Woodin, C.T.: *Effects of Dressing Parameters on Grinding Wheel Surface Topography*. Georgia Institute of Technology (2014)
- Wu, C.: Towards linear-time incremental structure from motion. In: 2013 International Conference on 3D Vision - 3DV 2013, 29 June–1 July 2013, pp 127–134 (2013). <https://doi.org/10.1109/3dv.2013.25>
- Xie, J., Xu, J., Tang, Y., Tamaki, J.: 3D graphical evaluation of micron-scale protrusion topography of diamond grinding wheel. *Int. J. Mach. Tools Manuf.* **48**(11), 1254–1260 (2008). <https://doi.org/10.1016/j.ijmachtools.2008.03.003>
- Yahyaoui, H., Ben Moussa, N., Braham, C., Ben Fredj, N., Sidhom, H.: Role of machining defects and residual stress on the AISI 304 fatigue crack nucleation. *Fatigue Fract. Eng. Mater. Struct.* **38**(4), 420–433 (2015). <https://doi.org/10.1111/ffe.12243>
- Zouhayar, A.-A., Naoufel, B.M., Houda, Y., Habib, S.: Surface integrity after orthogonal cutting of aeronautical aluminum alloy 7075-T651. In: *Design and Modeling of Mechanical Systems*, pp. 485–492. Springer, Heidelberg (2013)